Structures of Carbon Nanocrystals

John M. Cowley,[†,‡] Radhika C. Mani,[§] Mahendra K. Sunkara,*[,§]
Michael O'Keeffe,[||] and Charlotte Bonneau[||]

Department of Physics and Astronomy, Arizona State University, Tempe, Arizona 85287-1504, Department of Chemical Engineering, University of Louisville, Louisville, Kentucky 40292, and Department of Chemistry and Biochemistry, Arizona State University, Arizona 85287-1604

Received May 29, 2004. Revised Manuscript Received August 16, 2004

Single-crystal electron nanodiffraction patterns have been obtained from nanocrystals of various phases formed within carbonaceous balls produced by chemical vapor deposition (CVD). For the face-centered cubic phase, n-diamond, with cell dimension $a = 0.36$ nm, the relative intensities of the (200) reflection (forbidden for the diamond structure) and the (111) reflection suggest that the structure may include hydrogen atoms, and theoretical analyses support this possibility. There is evidence for a body-centered cubic phase with $a = 0.31$ nm, and the incorporation of hydrogen in this structure is suggested. Small amounts of hexagonal diamond, i-carbon, and other cubic phases are also present.

Introduction

It is known that carbon may occur in many different crystalline forms, beyond the well-known forms of diamond and graphite. The occurrence of hexagonal diamond (Lonsdaleite) has been known for many years.[1] At high temperatures and pressures, the various types of carbynes, chaoite, and carbon VI may be produced.[2] Recent observations of thin films of carbon formed by chemical vapor deposition (CVD),[3,4] plasma-chemical synthesis,[5] treatment of diamond surface with hydrogen plasma,[6] shock compression,[7] or ion implantation[8,9] have revealed the presence of a further range of crystalline forms. These include, in addition to the hexagonal diamond, a face-centered cubic form known as n-diamond, a further cubic form known as i-carbon, and other suggested forms, which are suspected but not well authenticated.

In this paper we report further investigations of such phases, formed by CVD, making use of electron nanodiffraction to obtain single-crystal electron diffraction patterns from individual nanocrystals, adding clarification to the partially known structures and suggesting the presence of further new structures.

The samples were obtained from carbonaceous balls formed on the ends of platinum wires immersed in a plasma in a microwave CVD reactor.[10] Diffraction patterns formed from the surfaces of the balls showed that the outer layers mostly consist of small, deformed crystals of graphite, which have favorable configurations for electrochemical purposes.[11] The fine powder formed by crushing the balls was shown by nanodiffraction to contain graphite crystals, amorphous carbon, and very small crystals of diamond-like phases, in confirmation of the deductions from Raman spectroscopy.[10] Further investigations of the diamond-like phases were then carried out using the nanodiffraction capabilities of a scanning transmission electron microscopy (STEM) instrument in which the incident beam of 100 keV electrons was focused to a diameter of less than 1 nm at the specimen level.[12]

The diffraction patterns came from crystals in arbitrary orientations. It is not feasible to tilt the nanocrystals into axial orientations, so that one had to accept the patterns that appeared as the incident was moved over the specimen. For most beam positions, the patterns showed only a few widely spaced spots, were not interpretable in terms of recognizable phases, and were not recorded. Those patterns showing regular two-dimensional arrays of spots were recorded. Most of these could be attributed to relatively simple cubic or hexagonal structures, including those previously identified from selected-area electron diffraction (SAED) ring patterns, as coming from the so-called n-diamond, i-carbon, or hexagonal diamond.

* Corresponding author. Phone: 502-852-1558. Fax: 502-852-6355. E-mail: mahendra@louisville.edu.
† Department of Physics and Astronomy, Arizona State University.
‡ Dedicated by his coauthors to the memory of John M. Cowley, FRS (1923−2004), formerly Galvin Professor of Physics, Arizona State University.
§ Department of Chemical Engineering, University of Louisville.
|| Department of Chemistry and Biochemistry, Arizona State University.

(1) Bundy, F. P.; Kasper, J. S. *J. Chem. Phys.* **1967**, *46*, 3437.
(2) Whittaker, A. G. *Science* **1978**, *200*, 763.
(3) Vora, H.; Moravec, T. J. *J. Appl. Phys.* **1981**, *52*, 6151.
(4) Rossi, M.; Vitali, G.; Terranova, M. L.; Sessa, V. *Appl. Phys. Lett.* **1993**, *63*, 2765.
(5) Jarkov, S. M.; Titarenko, Ya. N.; Churilov, G. N. *Carbon* **1998**, *36*, 595.
(6) Fatow, M.; Konyashin I.; Babaev V.; Guseva, M.; Khvostov, V.; Savtchenko, N. *Vacuum* **2002**, *68*, 75.
(7) Hirai, H.; Kondo, K. *Science* **1991**, *253*, 772.
(8) Prawer, S.; Peng, J. L.; Orwa, J. O.; McCallum, J. C.; Jamieson, D. N.; Bursill, L. A. *Phys. Rev. B* **2000**, *62*, R16360.
(9) Peng, J. L.; Bursill, L. A.; Jiang, B.; Orwa, J. O.; Prawer, S. *Philos. Mag. B* **2001**, *81*, 2071.
(10) Mani, R. C.; Sharma, S.; Sunkara, M. K.; Gullapalli, J.; Baldwin, R. P.; Rao, R.; Rao, A. M.; Cowley, J. M. *Electrochem. Solid−State Lett.* **2002**, *5*, E32.
(11) Mani, R. C.; Sunkara, M. K.; Baldwin, R. P.; Gullapalli, J.; Chaney, J. A.; Bhimarasetti, G.; Cowley, J. M.; Rao, R.; Rao, A. M. Submitted for publication.
(12) Cowley, J. M. *Microsc. Res. Tech.* **1999**, *46*, 75.

10.1021/cm0491429 CCC: $27.50
Published on Web 10/19/2004

The structure of the n-diamond is of particular interest. The patterns previously reported were SAED patterns coming from regions of diameter of the order of 100 nm and were ring patterns because the individual crystallites had dimensions of 10 nm or less but showed that the n-diamond has the same unit cell dimensions as normal diamond. However, the presence of strong (200), (222), and (420) reflections, forbidden for the normal cubic ($Fd\bar{3}m$) diamond structure, suggests that the symmetry is that of the $Fm\bar{3}m$ space group, i.e., a simple face-centered cubic (fcc) structure.[3−9] The analysis of the material by electron-energy-loss spectroscopy (EELS)[8,13] did not reveal the presence of any element besides carbon, leading to the assumption that the fcc cell, with $a = 0.356$ nm, contains only 4 carbon atoms, each with 12 nearest neighbors at a distance of 0.251 nm. This appears to be a surprising deviation from the bonding in any known carbon structure.

Initial theoretical analysis[13] suggested that for a fcc carbon structure the cell dimensions for maximum stability should be about 0.356 nm as observed. But later, more complete calculations[14] suggested that the most stable cell dimension would be 0.308 nm. Murrieta et al.[15] found that the energy shows a minimum for isotropic deformation at $a = 0.308$ nm, but the energy exhibits a maximum for tetragonal and trigonal deformations. They concluded that the fcc structure is not a true metastable phase but may possibly be stabilized by influence of a substrate or by impurities.

We have attempted to apply our observations of the single-crystal nanodiffraction patterns to resolve the mystery of this peculiar structure. We suggest the possibility of the incorporation of H in the structure, which would not be detected by EELS.

The so-called i-carbon is said to have a cubic structure with cell dimensions around 0.42 nm[7,8] although the possibility of a considerable range of cell dimensions, from 0.396 to 0.428 nm, has been reported.[3] A possible structure for this phase has been suggested by Matsushenko et al.[16] Another cubic phase formed at high pressure, with $a = 0.545$ nm, has been reported by Aust and Drickamer,[17] and Miki-Yoshida et al.[18] found a similar structure in heated soot.

Our observations suggest that there may also be a body-centered cubic (bcc) phase with cell dimensions about $a = 0.31$ nm.

Experimental Section

Platinum wires were immersed into a microwave plasma CVD reactor (ASTeX 5010) at a power of 1100 W, pressure 50 Torr, and gas composition of 1−2% CH_4/H_2.[10] During the experiments, the plasma tended to discharge at the tip of the metal wires, attaining very high temperatures, close to the melting point of platinum. Hence the tip balled-up, giving rise to a dense carbon deposition at the tip of the platinum wire substrate.

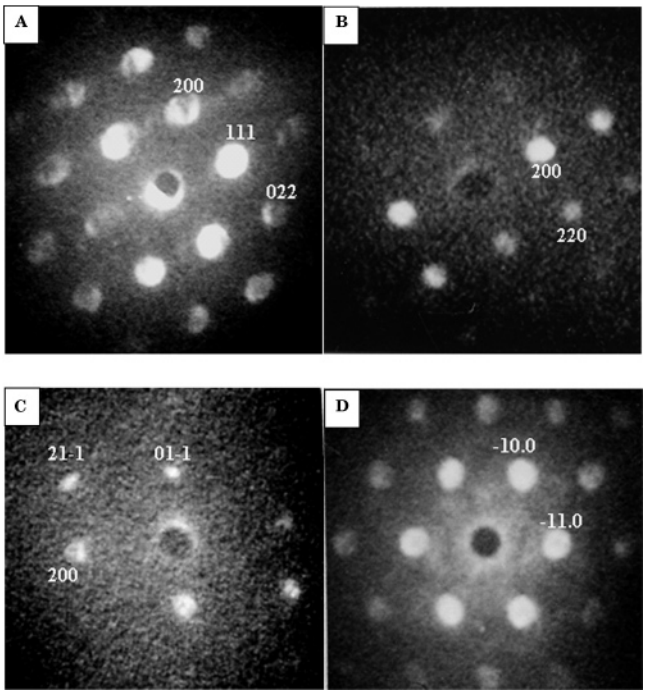

Figure 1. Electron nanodiffraction patterns for (A) face-centered-cubic crystal in [110] orientation, with the prominent (200)- and (111)-type reflections, (B) cubic crystal (fcc or bcc) in [100] orientation (indexed for fcc), (C) body-centered cubic structure in [110] orientation, and (D) hexagonal structure in [00.1] orientation or a cubic structure in [111] orientation giving a hexagonal pattern.

For the study of the diamond-like phases in the interior of the balls, the individual balls were crushed on a clean glass plate. The small particles were then mounted by adhesion to a copper or molybdenum electron microscopy grid. The usual amorphous carbon supporting films were not employed because such films can introduce confusion with the amorphous and other components of the specimen.

Electron nanodiffraction patterns were recorded with electron beams of 100 keV energy and a nominal width at the specimen level of 0.7 nm, using a STEM instrument from VG Microscope, Ltd. (Cambridge, U.K.). Low-magnification, point-projection ("shadow") images were used to locate suitable specimen areas, and when the beam was scanned over the specimen, bright-field images or dark-field images obtained with diffraction spots could be recorded, with an electronic marker to indicate the positions of the beam for which diffraction patterns were obtained.[12] Recording of the patterns was made by direct photography from a viewing screen or else by recording with a VCR for later photography. The latter means was well suited for obtaining series of patterns from adjacent regions during a slow scan of the incident beam or for recording transient patterns from regions subject to radiation damage.

Because the diffraction spots in nanodiffraction patterns tend to be rather large and often of irregular shape (see Figure 1), and because of difficulties with the calibration of the instrument, the accuracy for the determination of lattice spacing was rarely better than a few percent. However, this limited accuracy was sufficient to distinguish the various phases.

Results

More than half of the nanodiffraction patterns from the crushed samples could clearly be attributed to graphite. For orientations almost perpendicular to the *c*-axis, the strong rows of spots corresponding to the *c*-spacing of 0.67 nm were prominent. With the beam parallel to the *c*-axis, the hexagonal spot pattern was

(13) Konyashin, I.; Zern, A.; Mayer, J.; Aldinger, F.; Babaev, V.; Khvostov, V.; Guseva, M. *Diamond Relat. Mater.* **2001**, *10*, 99.
(14) Pickard, C. J.; Milman, V.; Winkler, B. *Diamond Relat. Mater.* **2001**, *10*, 2225.
(15) Murrieta, G.; Tapia, A.; Coss, R. d. *Carbon* **2004**, *42*, 771.
(16) Matyushenko, N. N.; Strel'nitskii, V. E.; Gusev, V. A. *Sov. Phys. Crystallogr.* **1981**, *26*, 274.
(17) Aust, R. B.; Drickamer, H. G. *Science* **1963**, *140*, 817.
(18) Miki-Yoshida, M.; Rendon, L.; Jose-Yacaman, M. *Carbon* **1993**, *31*, 843.

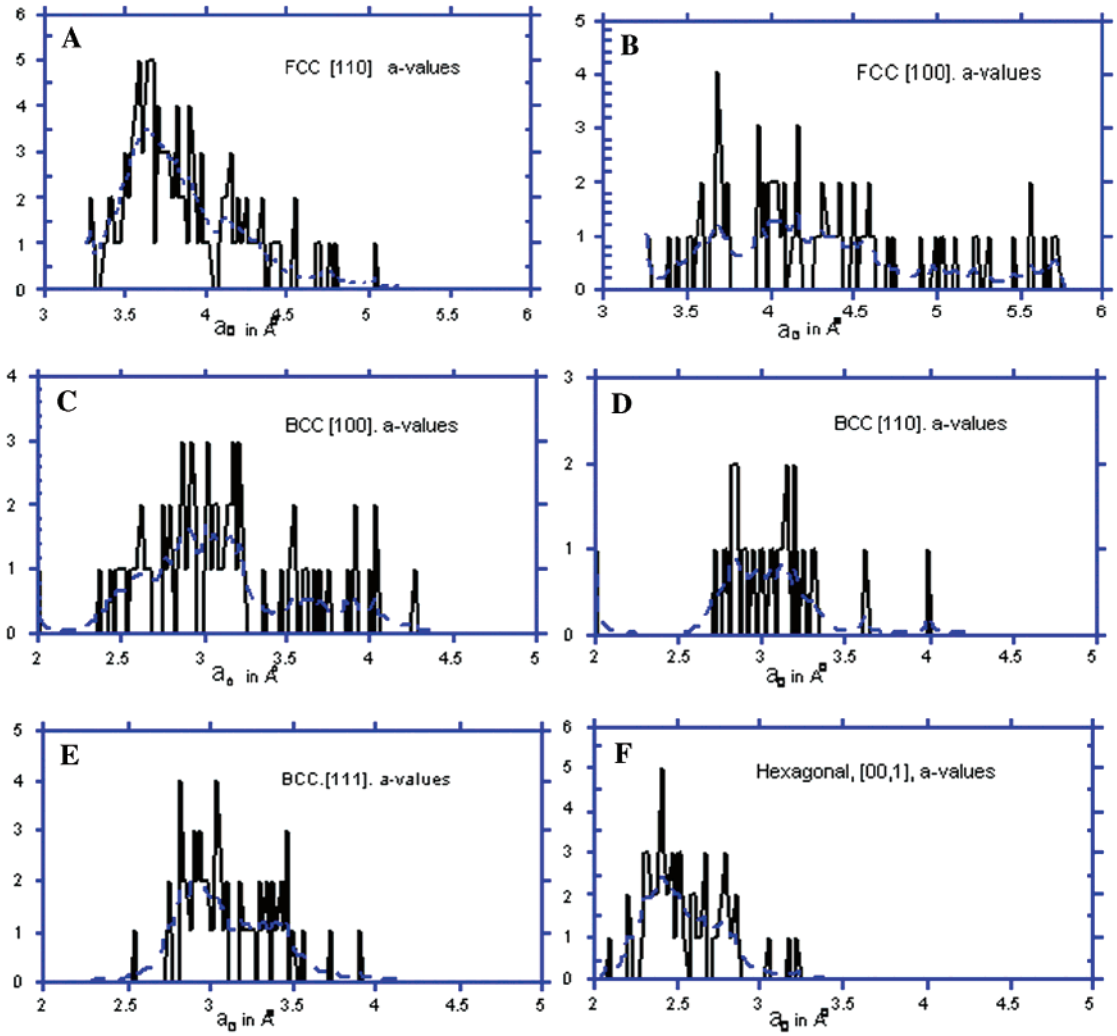

Figure 2. Diagrams showing the number of observations plotted against unit-cell dimensions (a-values) for (A) fcc [110], (B) fcc [100], (C) bcc [100], (D) bcc [110], (E) bcc [111], and (F) hexagonal [001]. The dashed curves result from smoothing to take account of the probable experimental error.

readily identified by the characteristic intensity distribution with the (10,0) spots much weaker than the (11,0). The graphite crystallites were often seen to be immersed in amorphous carbon.

Of the single-crystal diffraction patterns from other phases, the most common patterns were as follows:

(1) The typical patterns were from fcc in [110] orientation with strong (111)- and (200)-type spots, as in Figure 1A. Those corresponding to unit cell dimension $a = 0.36$ nm were attributable to n-diamond. Some with $a = 0.42$ nm could come from i-carbon. Figure 2A shows the numbers of such patterns recorded for the various a-values.

(2) Square patterns of spots were seen such as that in Figure 1B, which could come from cubic structures in [100] orientation. Figure 2B shows the numbers of these patterns recorded for various a-values, on the assumption of a fcc lattice, and Figure 2C shows the distribution on the assumption of a bcc lattice.

In Figure 2B the patterns with dimensions close to 0.36 nm could come from a fcc lattice (n-diamond) or a bcc lattice with $a = 0.25$ nm. The group of patterns with approximately $a = 0.42$ nm could come from i-carbon or from a bcc cell with $a = 0.3$ nm (see Figure 2C). There is a small group of patterns with dimensions corresponding to fcc with about 0.39 nm. Crystals with greater a-values may come from other phases such as that with $a = 0.55$ nm described by Aust and Drickamer.[17]

In Figure 2C, the peaks at 0.25 and 0.29 nm could come from the fcc structures with $a = 0.36$ and 0.41 nm, and the peaks at about 0.35 and 0.39 nm could come from fcc structures with about 0.5 and 0.55 nm. The main peak at about 0.31 nm can be attributed to a bcc structure only, because it appears in Figure 2D,E.

(3) Rectangular patterns are found, with principal dimensions in the ratio of the square root of 2, as in Figure 1C. These can be attributed to a bcc structure with $a = 0.3$ nm, approximately. The distribution of unit cell a-values for bcc structures in [110] orientation is shown in Figure 2D.

(4) Hexagonal patterns, such as that in Figure 1D, are clearly distinct from the hexagonal patterns from graphite in that the (10,0) and (11,0) spots are of comparable intensity. The observed distribution of lattice parameters, a-values for a hexagonal cell, is shown in Figure 2F. Such patterns could also be attributed to cubic unit cells in [111] orientation. If they are assigned to a bcc cell in [111] orientation, the distribution of observed a-values is as shown in Figure 2E. The main

peak of Figure 2E, at about 0.3 nm, corresponds to the main peak of Figure 2F, at about 0.25 nm (the value for hexagonal diamond). There is an uncertainty, therefore, as to the relative amounts of the bcc structure in [111] orientation and the hexagonal structure in [00,1] orientation.

The appearance of a subsidiary peak at about 0.34 nm in Figure 2E and the equivalent 0.28 nm in Figure 2F has not been interpreted. This is equivalent to the 0.35 nm peak visible in Figure 2C but only weakly present in Figure 2D.

(5) Patterns showing rows of closely spaced spots that may arise from structures with one long axis, such as the 0.67 nm of the *c*-axis of graphite. A few larger values observed are attributed to unknown impurities. A small number of patterns showed values around 0.41 nm, coming presumably from hexagonal diamond. It would be expected that the number of these patterns, produced with beam directions approximately perpendicular to the *c*-axis, would be comparable with the number of hexagonal patterns obtained from hexagonal diamond ($a = 0.252$ nm). Hence, it is suggested that most of the main peak in Figure 2F comes from bcc in [111] orientation.

The conclusion to be drawn from these data on lattice dimensions is that the most common phase present is the fcc n-diamond. Other phases include the i-carbon, a bcc phase with cell dimension approximately 0.31 nm, a small amount of hexagonal diamond, and possible small amounts of other phases.

n-Diamond Phase. This phase has been reported by many authors but appears to have a simple fcc structure, as suggested by the presence of the reflections (200), (222), and (420) which are forbidden for normal diamond. The implication is that there are only 4 carbon atoms in the unit cell instead of the 8 for diamond. We have attempted to clarify this extraordinary situation by observing the relative intensities of the spots in the nanodiffraction patterns. Because the nanocrystals occur in random orientation, the relative intensities of the spots in the patterns may vary widely with the tilt of the crystal with respect to the incident beam direction, but observations of relative intensities for recognizable two-dimensional patterns obtained close to a zone-axis orientation should give significant information.

Figure 3A shows the relative intensities of the (200) and (111) spots in patterns obtained from [110] orientation of fcc crystals with cell dimensions close to $a = 0.36$ nm. The intensities are approximate, estimated visually with the help of a calibration pattern formed by multiple exposures, but should be accurate to within about 20%. Figure 3B shows similar estimates of relative intensities of the (200) and (220) spots for fcc crystals with cell dimensions close to 0.36 nm in the [100] orientations.

For both the [110] and [100] orientations, the (200) intensities and the corresponding ratios are zero for normal diamond for diffraction with the usual assumption of kinematical scattering. For the assumed fcc structure of n-diamond, the (200) reflections would be quite strong with intensity ratios, for the axial orientations, as indicated in the diagrams. For the fcc structure, one would expect a broad distribution of values of the ratios around the value of the ratio for the axial orientation. Clearly, the distributions are not centered

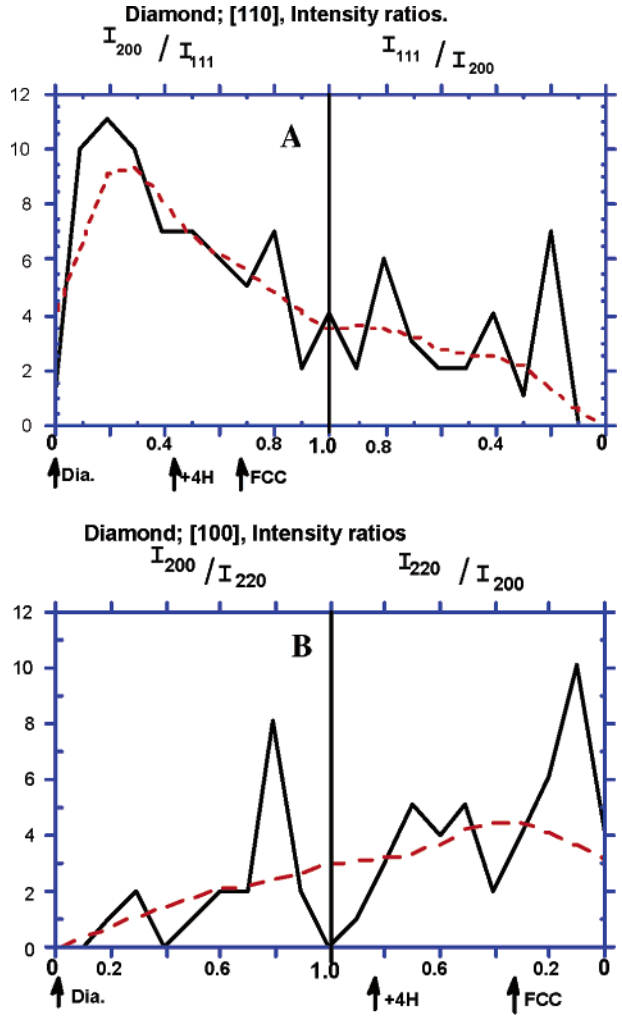

Figure 3. Plots of the number of observations of relative intensities in nanodiffraction patterns for the n-diamond structure ($a = 0.36$ nm): (A) ratios of intensities of (200) and (111) reflections for fcc [110] patterns; (B) ratios of intensities of (200) and (220) reflections for fcc [100] patterns. In each case, the ratios for the weaker (200) reflection are given on the left side and the ratios for the stronger (200) reflections are given on the right side.

on the values for the axial orientations of the fcc structure but appear to be centered about some value intermediate between that for the fcc structure and the zero values expected for normal diamond.

The deviation from the diamond values is emphasized by the observation of many patterns for which the (200) reflection is much stronger than (111). This could be expected for a fcc structure for particular tilts of the crystal but is very unlikely if the (200) intensity for the axial orientation is very much weaker than (111).

It is well-known that the intensities of electron diffraction single-crystal patterns may be strongly affected by dynamical scattering except for very small crystal thicknesses with only light atoms. Calculations of intensities for diamond crystals of increasing thickness were made using the multislice programs for dynamical scattering using the software MacTempas (developed by Roar Kilaas, NCEM, Berkeley, CA). The crystal size and beam voltage assumed for these calculations are 50 nm and 200 keV. In Figure 4A the calculated intensities of the (200) and (111) for the diamond structure are plotted against thickness for the

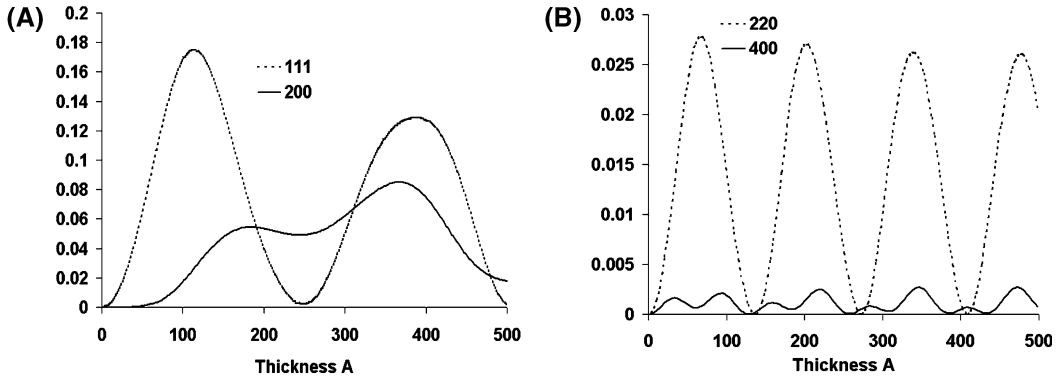

Figure 4. Dynamical diffraction calculations for intensities from diamond in (A) [110] and (B) [100] orientations as a function of crystal thickness. For the [100] orientation, the (200) intensity is close to zero for all thickness.

[110] orientation, and in Figure 4B, a similar plot is given for the [100] orientation. It is evident that for the [110] orientation the forbidden (200) reflection may be produced by dynamical scattering effects, but the (200) intensity is very small compared with the dominant (111) reflection for thickness of less than 10 nm. For the [100] orientation, the (200) reflection never gains appreciable intensity.

The thickness of the nanocrystals in our specimens could not be measured directly. Only the lateral extent of the nanocrystals can be seen in dark-field STEM images, but it may be assumed that, for randomly oriented crystals, the thickness is, on the average, approximately equal to the lateral dimensions. For most sample areas, the lateral dimensions of the coherently diffracting regions were seen in the dark-field STEM images to be in the range of 5−10 nm. Occasionally, larger crystals, up to 100 nm in diameter, which appeared to be in the form of thin sheets with numerous structural imperfections, were visible. As well as could be judged, the relative intensities of the diffraction spots from these larger crystals were the same as for the nanocrystals. Attempts were made to observe the variation of the relative intensities as the incident beam was translated across a thin edge of a larger crystal, but it was not possible to detect any variation of relative intensities with the assumed increase of thickness. It was therefore concluded that dynamical scattering effects were not an important factor for the interpretation of the relative spot intensities.

It is also known that forbidden reflections may appear in single-crystal patterns as a result of finite crystal dimensions or the presence of stacking faults or other defects of the crystal. Some calculations made for thin crystals with stacking faults as well as with mixed sp^2 and sp^3 bonding have failed to indicate the production of the forbidden (200) reflection with any but very small intensity.

Possible bcc Phase. It has been pointed out that the square patterns of spots from cubic structures in [100] orientation may be interpreted as coming from either fcc or bcc structures. Similarly, the hexagonal spot patterns may be interpreted as coming from either hexagonal structures in [00,1] orientation or from bcc (or fcc) structures in [111] orientations. However, only bcc structures in [110] orientation can give the rectangular patterns such as Figure 2C, and the fact that peaks appear for approximately the same a-values in Figure 2C−E is strongly suggestive of the presence of a bcc phase with approximately $a = 0.31$ nm.

The relative intensities in these patterns that may be attributed to this bcc phase do not show any pronounced features that would imply any great deviation from a simple bcc structure. The implication (subject to further discussion) is that the patterns come from a bcc carbon structure, with two carbon atoms in a unit cell with $a = 0.31$ nm. The C−C distance for the 8 nearest neighbors would then be 0.27 nm.

Incorporation of Hydrogen. The accepted structure for n-diamond, and also the suggested bcc structure, seem to involve such unprecedented bonding arrangements for carbon atoms that it is inevitable that the possibility of the presence of other atoms should be explored. However, attempts to detect other atoms in n-diamond samples by use of EELS have not been successful.[8,13] Since the only atom, which cannot be readily detected by EELS, is hydrogen, the presence of H in the structure must be considered.

The syntheses of n-diamond, in most cases, have been made in the presence of hydrogen. Theoretical studies of carbon clusters have suggested that hydrogen may have an essential role in bonding at least on the surfaces of the stable clusters[19] and the similar roles for hydrogen have been postulated for the explanation of some experimental observations.[8,9]

We have therefore investigated the possibility of the incorporation of H in the structure of n-diamond. The normal diamond structure may be described as consisting of two intergrown fcc structures, with origins at the positions 0, 0, 0 and 1/ 4, 1/4, 1/4. If one assumes that the 4 carbon atoms on one of these substructures are replaced by hydrogen atoms, the unit cell content is C_4H_4 and the symmetry is fcc, as for the zinc blende structure. The relative intensities of the (200) and (111) reflections and of the (200) and (220) reflections are as indicated by the arrows labeled "+4H" in Figure 3A,B. These relative intensity values provide a better account of the distributions of relative intensities than those for either the normal diamond or the pure carbon fcc structures, although some structure a little closer to that of the normal diamond structure (i.e. with a little more scattering power than 4 H on the one sublattice) may give an even better fit.

(19) Ree, F. H.; Winter, N. W.; Glosli, J. N.; Viecelli, J. A. *Physica B* **1999**, *265*, 223.

Table 1. Calculated Values for the Unit Cell Dimension and the Energy/Carbon Atom, ΔE/C, for Various Possible CH_x Phases

composn	symm	struct	a (Å)	ΔE_f/C (eV)
C	$Fm\bar{3}m$	fcc	3.098	4.61
CH	$F\bar{4}3m$	ZnS	3.583	5.21
CH_2	$Fm\bar{3}m$	CaF_2	3.787	5.64
CH_3	$Fm\bar{3}m$	a	3.953	5.75
C	$Im\bar{3}m$	bcc	2.389	4.43
CH_2	$Pn\bar{3}m$	Cu_2O	3.107	3.64
CH_3	$Pm\bar{3}n$	A15	3.096	7.20
CH_4	$Im\bar{3}m$	b	3.326	4.22

[a] C, 0, 0, 0; H, 1/2, 1/2, 1/2 and 1/4, 1/4, 1/4. [b] C, 0, 0, 0; H, 1/4, 1/4, 1/4.

To provide some further foundation for the suggestion of such a structure, a theoretical analysis was carried out.

Theoretical Studies. Our calculations have been carried out using density functional theory[20,21] with the gradient-corrected local exchange-correlation potential of Perdew and Wang.[22,23] We used the VASP code.[24,25] We employed standard periodic boundary conditions with the core electrons represented by ultrasoft pseudopotentials[26] and a plane-wave basis set for the valence electrons. A plane-wave cutoff of 500 eV was found to be sufficient to converge total energies and geometries. k-point sampling during geometry optimization for all structures was carried out on a $11 \times 11 \times 11$ Monkhort−Pack grid.[27] Geometry optimization was undertaken using a combination of conjugate gradient (first derivative) and quasi-Newton (approximate second derivative) methods.

There have been a number of calculations of the properties of fcc C; our unit cell parameter $a = 3.098$ Å is in good accord with previous results (3.020−3.082 Å).[14,15] For bcc C we find $a = 2.389$ Å. We note however that there is strong evidence that these phases are mechanically unstable at least at low pressure.[15,28]

The fact that the unit cell parameters have a wide range of values suggest very strongly that we are dealing with a phase of variable composition, and the most plausible candidate is CH_x. Accordingly we examined a number of compositions with either fcc C or bcc C (Table 1). As can be seen from Table 1, the unit cell edge increases smoothly from C to CH_3 (fcc) and from C to CH_3 (bcc) in most cases. Notice that the most stable phase is the "bcc" CH_2 with $a = 3.107$ Å. This phase actually has a positive affinity for H_2, i.e., for the reaction $CH_2 \rightarrow C + H_2$, $\Delta E = 0.72$ eV. We also find that in contrast to the pure carbon phase this phase is at a local minimum of energy (metastable).

It was determined that for H on one of the diamond sublattices, such that the unit cell contained 4 C and 4 H, the equilibrium unit cell dimension would be 0.358 nm. This in agreement with the observations and distinctly different from the value 0.307 nm for vacancies in place of the hydrogen atoms (in agreement with result of Pickard et al.[14] and Murrieta et al.[15]).

A further result is that, for the CH_2 structure, the equilibrium unit cell dimension would be 0.379 nm. The plots of Figure 2A,B suggest that a minor peak is present at about this value.

Discussion

An independent confirmation of the presence of H in the n-diamond structure would be desirable. However, no known technique other than electron nanodiffraction seems to be available. Any technique for which the volume of the sample examined has dimensions greater than about 10 nm would not be successful for our samples since the nanocrystals of n-diamond are mostly embedded in amorphous carbon and accompanied by crystals of other phases including graphite. The EELS technique has the required spatial resolution but is not sensitive to hydrogen.

An alternative model for the n-diamond structure, not involving H, has been proposed by Hirai et al.[29] However, their structures involve peculiar bonding configurations and, for their most favored model, the calculated diffraction intensities are in poor agreement with our observations.

The calculations have shown that the proposed CH_2 bcc is metastable with $a = 0.31$ nm, as observed. The relative intensities of the bcc diffraction spots would be modified by the inclusion of the H atoms, but the differences would be difficult to confirm for the nanocrystals in random orientation. Some fcc reflections, such as the (111), would appear weakly. Such reflections, too weak for reproduction, have been observed in a few of the bcc [110] patterns. An alternative structure could be one in which 2 H atoms are included in each bcc unit cell, at the positions 1/4, 1/4, 1/4 and 3/4, 3/4, 3/4. Then no fcc-type reflections would appear. The unit cell would tend to be distorted to become rhombohedral. A small distortion of this type would not easily be detected in the nanodiffraction patterns.

For the proposed bcc structure the insertion of four hydrogen atoms would give a tetrahedral coordination for the C atoms with a C−H distance of about 0.14 nm, as against 0.16 nm for the fcc structure which has 8 nearest-neighbor C−H bonds.

The crystalline phases involving CH_x found at the nanoscale could possibly act as intermediate phases prior to diamond nuclei formation and, hence, may explain the pathway for diamond nucleation. This hypothesis extends the existing theories for diamond nucleation.[30,31]

Conclusions

In conclusion, we have shown evidence that, for the n-diamond, the simple fcc structure with just 4 C in a unit cell seems unlikely. Our suggestion for the incor-

(20) Hohenburg, P.; Kohn, W. *Phys. Rev.* **1964**, *136*, B864.
(21) Kohn, W.; Sham, L. J. *Phys. Rev.* **1965**, *140*, A1133.
(22) Perdew, J. P.; Zunger, A. *Phys. Rev. B* **1981**, *23*, 5048.
(23) Perdew, J. P.; Wang, Y. *Phys. Rev. B* **1992**, *46*, 12947.
(24) Kresse, G.; Furthmüller, J. *Phys. Rev. B* **1996**, *54*, 11169.
(25) Kresse, G.; Furthmüller, J. *Comput. Mater. Sci.* **1996**, *6*, 15.
(26) Vanderbilt, D. *Phys. Rev. B* **1990**, *41*, 7892.
(27) Monkhorst, H. J.; Pack, J. D. *Phys. Rev. B* **1976**, *13*, 5188.
(28) Mailhiot, C.; McMahan, A. K. *Phys. Rev. B* **1991**, *44*, 11578.
(29) Hisako, H.; Kondo, K.; Sugiura, H. *Appl. Phys. Lett.* **1992**, *61*, 414.
(30) Lambrecht, W. R. L.; Lee, C. H.; Segall, B.; Angus, J. C.; Li, Z. D.; Sunkara, M. K. *Nature* **1993**, *364*, 607.
(31) Lifshitz, Y.; Kohler, T.; Frauenheim, T.; Guzmann, I.; Hoffman, A.; Zhang, R. Q.; Zhou, X. T.; Lee, S. T. *Science* **2002**, *297*, 1531.

poration of H in the lattice is supported experimentally and theoretically. It leads to a seemingly improbable structure but one that is less improbable than the structure without H. The proposed existence of a bcc structure with the addition of hydrogen and $a = 0.31$ nm may also seem improbable but is even more strongly supported theoretically.

We note that the proposed structures containing hydrogen involve a very high density of hydrogen atoms suggesting their possible interest as hydrogen-storage media. These crystalline metastable CH_x phases could explain the intermediate structures that might be present during diamond nucleation.

Acknowledgment. The specimen preparation was made with support from the National Science Foundation Grant CTS 9876251. The nanodiffraction observations were made with the support of the ASU Center for High Resolution Electron Microscopy. The authors also gratefully acknowledge support from NSF Grant DMR 0103036.

CM0491429